Available online at www.sciencedirect.com

SCIENCE DIRECT

Biochimica et Biophysica Acta 1665 (2004) 48–56

BIOCHIMICA ET BIOPHYSICA ACTA

BBA

http://www.elsevier.com/locate/bba

OVCAR-3 cells internalize TAT-peptide modified liposomes by endocytosis

Marjan M. Fretz[a,*], Gerben A. Koning[a,b], Enrico Mastrobattista[a], Wim Jiskoot[a], Gert Storm[a]

[a]*Department of Pharmaceutics, Utrecht Institute for Pharmaceutical Sciences (UIPS), Utrecht University, P.O. Box 80082, 3508 TB Utrecht, The Netherlands*
[b]*Department of Radiochemistry, Interfaculty Reactor Institute, Delft University of Technology, Mekelweg 15, 2629 JB Delft, The Netherlands*

Received 20 April 2004; received in revised form 23 June 2004; accepted 24 June 2004
Available online 30 July 2004

Abstract

For cytosolic delivery of liposomes containing macromolecular drugs, such as proteins or nucleic acids, it would be beneficial to bypass endocytosis to prevent degradation in the lysosomes. Recent reports pointed to the possibility that coupling of TAT-peptides to the outer surface of liposome particles would enable translocation over the cellular plasma membrane.

Here, we demonstrate that cellular uptake of TAT-liposomes occurs via endocytosis rather than plasma membrane translocation. The coupling of HIV-1 derived TAT-peptide to liposomes enhances their binding to ovarian carcinoma cells. The binding was inhibited by the presence of heparin or dextran sulfate, indicating that cell surface proteoglycans are involved in the binding interaction. Furthermore, *living* confocal microscopy studies revealed that binding of the TAT-liposomes to the plasma membrane is followed by intracellular uptake in vesicular structures. Staining the endosomes and lysosomes demonstrated that fluorescent liposomal labels are present within the endosomal and lysosomal compartments. Furthermore, incubation at low temperature or addition of a metabolic or an endocytosis inhibitor blocked cellular uptake.

In conclusion, coupling TAT-peptide to the outer surface of liposomes leads to enhanced endocytosis of the liposomes by ovarian carcinoma cells, rather than direct cytosolic delivery by plasma membrane translocation.

Keywords: Liposome; TAT-peptide; Endocytosis; Proteoglycans; Translocation

1. Introduction

Unfavorable physicochemical characteristics of therapeutic macromolecules, like nucleic acids, proteins and peptides, generally limit their application as agents, e.g. for cancer therapy. Due to their large molecular weight, hydrophilicity and charged nature, these molecules are inefficient in crossing cellular membranes and therefore in reaching their intracellular target site [9]. Therefore, intracellular delivery of these novel biopharmaceuticals rely on delivery systems that allow improved transport across the cell membrane. Currently, attempts are being made to apply targeted liposomes for cytosolic delivery of macromolecules [14,28,29]. However, cytosolic delivery of liposome-encapsulated drugs is often not accomplished as binding of liposomes to the targeted cell surface receptor is followed by endocytic uptake and subsequent lysosomal degradation of the liposomes with their encapsulated contents.

A recently reported approach to avoid endocytosis and to achieve direct cytosolic delivery of poor membrane permeable (macro) molecules is to utilize so-called cell-penetrating peptides (CPP) (also referred to as protein transduction domains), which have been described to possess the ability to translocate material across the plasma membrane into the cytoplasm (reviewed in Refs. [11,18]). These peptides can act as cytosolic delivery vectors for both low and high molecular weight cargos, like FITC [30], proteins [4,15,24], oligonucleotides [1] and even particulates [10,25,26].

* Corresponding author. Tel.: +31 30 253 6899; fax: +31 30 251 7839.
E-mail address: m.m.fretz@pharm.uu.nl (M.M. Fretz).

0005-2736/$ - see front matter © 2004 Elsevier B.V. All rights reserved.
doi:10.1016/j.bbamem.2004.06.022

Torchilin et al. [25] were the first to report on cytosolic delivery of liposomes modified with a CPP (the HIV-1-derived TAT-peptide) attached directly to the outer liposomal surface or to the terminal ends of PEG-chains present on PEG-coated liposomes. The latter PEG-liposomes, also known as sterically stabilized liposomes, are advantageous in vivo because of their prolonged circulation property. The TAT-liposomes were delivered into the cytoplasm via an energy-independent uptake mechanism as concluded from the observations that no significant reduction in cellular uptake occurred when incubated at 4 °C instead of 37 °C or in the presence of metabolic inhibitors [25]. Therefore, translocation into the cytoplasm rather than endocytosis was proposed as cellular uptake mechanism. Similar results on CPP-mediated liposomal translocation were published by Tseng et al. [26].

In the meantime, the concept of CPP-mediated plasma membrane translocation was questioned when Lundberg and Johansson [12] showed that cell fixation techniques could induce rigorous artifacts in the cellular distribution of fluorescently labeled CPP. In addition, Richard et al. [19] reported on characteristic endosomal localization of fluorescently labeled CPP when cell fixation was avoided, as visualized by living cell fluorescence microscopy. Moreover, the cellular uptake kinetics of CPP appeared to be similar to the kinetics of endocytosis and cellular uptake did not occur at 4 °C. These observations argue for an energy-dependent uptake process and have raised serious doubts about the translocation mechanism of cellular entry.

Here, we have studied the cellular uptake mechanism of TAT-liposomes by living unfixed human ovarian carcinoma cells (OVCAR-3), thus avoiding possible fixation-induced artifacts. The results clearly indicate that TAT-mediated uptake of liposomes occurs via endocytosis, rather than via plasma membrane translocation as previously proposed.

2. Experimental methods

2.1. Materials

Egg-phosphatidylcholine (EPC) and 1,2-distearoyl-glycero-3-phosphoethanolamine-*N*-[poly(ethylene glycol)2000] (PEG_{2000}-DSPE) were obtained from Lipoid GmbH (Ludwigshafen, Germany). Maleimide-PEG_{2000}-DSPE was obtained from Shearwater Polymers (Huntsville, AL, USA). Cholesterol (CHOL), iodoacetamide, cytochalasin D, heparin, dextran sulfate and FITC-dextran (molecular mass 77 kDa) were from Sigma-Aldrich Co. (St. Louis, MO, USA). 1,1′-Dioctadecyl-3,3,3′,3′-tetramethylindocarbocyanine, 4-chlorobenzenesulfonate sulfonate salt (DiD) and Lysotracker Red DND-99 were purchased from Molecular Probes Europe BV (Leiden, The Netherlands). Lissamine rhodamine B-labeled glycerophosphoethanolamine (Rho-PE) was obtained from Avanti Polar Lipids Inc. (Alabaster, AL, USA). Titriplex III (EDTA) was obtained from Merck (Darmstadt, Germany). Thiol-acetylated TAT-peptide with the sequence YGRKKRRQRRRK-S-acetylthioacetyl was synthesized by Ansynth BV (Roosendaal, The Netherlands).

2.2. Cell culture

The human ovarian carcinoma cell line NIH:OVCAR-3 originates from the laboratory of Dr. Hamilton (National Cancer Institute, Bethesda, MD) [6]. OVCAR-3 cells were cultured in Dulbecco's modified Eagle's medium containing 3.7 g/l sodium bicarbonate, 4.5 g/l L-glucose and supplemented with L-glutamine (2 mM), 10% (v/v) fetal calf serum (FCS), penicillin (100 IU/ml), streptomycin (100 μg/ml) and amphotericin B (0.25 μg/ml) at 37 °C with 5% CO_2 in humidified air.

All cell culture-related material was obtained from Gibco (Grand Island, NY, USA).

2.3. Liposome preparation and characterization

For the preparation of liposomes, a lipid film was prepared from a mixture of EPC, CHOL, PEG_{2000}-DSPE, maleimide-PEG_{2000}-DSPE (1.85:1:0.09:0.06 molar ratio) in absolute ethanol by solvent evaporation. DiD or Rho-PE (0.1 mol%) was added as lipophilic fluorescent label. Before hydration, the lipid film was flushed with nitrogen for at least 30 min. Liposomes were formed by hydration of the lipid film with either Hepes buffered saline (150 mM NaCl, 5 mM Hepes, pH 6.5; HBS) or HBS (pH 6.5) containing 10 mg/ml FITC-dextran. The lipid dispersion was sequentially extruded through polycarbonate membrane filters (Osmonic, Livermore, CA, USA) with pore sizes varying from 0.05 to 0.65 μm using Lipex high-pressure extrusion equipment (Northern Lipids, Vancouver, Canada).

When hydrated with FITC-dextran-containing solution, the non-encapsulated FITC-dextran was separated from the liposomes by size exclusion chromatography using a Sepharose CL-4B column (Amersham Pharmacia Biotech, Uppsala, Sweden).

TAT-peptides were covalently coupled to the maleimide-derivatized PEG-DSPE present in the liposomal bilayer via a sulfhydryl-maleimide coupling reaction as previously described for monoclonal antibodies [7]. Briefly, 1 mg of thiol-acetylated peptide was deacetylated in an aqueous solution containing 0.5 M Hepes, 0.5 M Hydroxylamine-HCl and 0.25 mM EDTA of pH 7.0 for 1 h at room temperature to obtain free sulfhydryl groups. The deacetylated peptide was added to liposomes (21 μmol total lipid) and the coupling reaction to the maleimide functionalized PEG chains present on the surface of the liposomes, was performed overnight at 4 °C. The non-coupled peptide was removed by size exclusion chromatography using a Sepharose CL-4B column. As control, liposomes lacking the TAT-peptide were used.

The phospholipid concentration of the liposome formulations was determined by the colorimetric method of

Rouser et al. [20]. Mean particle size and size distribution were determined by dynamic light scattering with a Malvern 4700 system (Malvern Ltd., Malvern, UK).

2.4. Cellular association

OVCAR-3 cells were detached from the culture flask by trypsin/EDTA solution (0.05% (w/v) trypsin and 0.02% (w/v) EDTA in PBS). Cells (1×10^5) were incubated for 1 h at 4 °C with different concentrations Rho-PE labeled control liposomes or TAT-liposomes. Cells were washed twice by centrifugation ($300\times g$, 5 min, 4 °C) and addition of 1 ml PBS (164 mM NaCl, 140 mM Na_2HPO_4, 11 mM NaH_2PO_4; pH 7.4). After centrifugation, the cells were resuspended in 400 μl PBS and analyzed by flow cytometry using a FACSCalibur (Becton&Dickinson, Mountain View, CA, USA).

2.5. Fixation-induced artifact

OVCAR-3 cells were seeded (2×10^4 cells/well) onto 16-well chamber slides and cultured overnight prior to the experiment. Cells were washed with PBS and 150 nmol Rho-PE labeled liposomes (control or TAT-liposomes) in serum-free medium was added. After 1 h, the unbound liposomes were removed and the cells were washed with PBS. The cells were either mounted in PBS and directly visualized by confocal microscopy or fixed with 4% formaldehyde and mounted in FluorSave reagent (Calbiochem, San Diego, CA, USA) before visualization. The confocal microscopy analysis was performed with a Leica TCS-SP confocal laser scanning microscope equipped with a 488 nm Argon, 568 nm Krypton and 647 nm HeNe laser. Laser power and photomultiplier settings were kept identical for all the samples to be able to compare the results.

2.6. Intracellular localization

OVCAR-3 cells were seeded (2×10^4 cells/well) onto 16-well chamber slides and cultured overnight prior to the experiment. Cells were washed with PBS and 150 nmol double fluorescently labeled (DiD as lipophilic bilayer label and FITC-dextran as aqueous marker) control or TAT-liposomes in serum-free medium was added. After 1 h, the unbound liposomes were removed and the cells were subsequently incubated for either 1 or 23 h with culture medium. Thirty minutes prior to visualization the cells were incubated with 100 μl Lysotracker Red solution (75 nM in PBS) at 37 °C. Cells were washed with PBS, mounted in PBS and covered with cover slip sealed with nail polish. The living cells were directly analyzed with a Leica TCS-SP confocal laser scanning microscope equipped with a 488 nm argon, 568 nm krypton and 647 nm HeNe laser. Laser power and photomultiplier settings were kept identical for all the samples to be able to compare the results.

2.7. Cellular association in the presence of inhibitors

OVCAR-3 cells were detached by trypsin/EDTA solution and 3×10^5 cells/well were added to six wells CoStar low-adherence plates (Corning Life Science BV, Schiphol-Rijk, The Netherlands) in a total volume of 5 ml serum-free medium. The experiments were performed at 4 and 37 °C with or without the presence of 1 mM iodoacetamide or 25 μg/ml cytochalasin D. In each well, 450 nmol Rho-PE labeled liposomes (TAT or control liposomes) was added and after incubation for 5 h, the cells were washed twice by centrifugation ($300\times g$, 5 min, 4 °C) and resuspended in PBS. An aliquot of the cell suspension was mounted on glass slides and visualized directly using a Leica TCS-SP confocal laser scanning microscope equipped with 568 nm krypton laser. Laser power and photomultiplier settings were kept identical for all the samples to be able to compare the results. Cell samples were also analyzed by flow cytometry using a FACSCalibur (Becton&Dickinson).

2.8. Cellular association in the presence of heparin and dextran sulfate

OVCAR-3 cells were detached from the culture flask by trypsin/EDTA solution. Cells (1×10^5) were incubated for 1 h at 4 °C with 150 nmol Rho-PE labeled TAT-liposomes in the presence of different concentrations of heparin or dextran sulfate. Cells were washed twice by centrifugation ($300\times g$, 5 min, 4 °C) and addition of 1 ml PBS. Cells were resuspended in 400 μl PBS and analyzed by flow cytometry using a FACSCalibur (Becton&Dickinson).

3. Results

3.1. Liposome characterization

Liposomes composed of EPC, CHOL, PEG_{2000}-DSPE and maleimide-PEG_{2000}-DSPE (1.85:1:0.09:0.06 molar ratio) were prepared according to the evaporation/hydration method and the liposomes were reduced in size by extrusion [16]. After extrusion, the activated TAT-peptide was coupled to the maleimide functionalized PEG-DSPE on the outer liposomal surface as described in Experimental methods. The type of fluorescent label, mean particle size and size distribution of the used liposomal formulations are given in Table 1. The liposomes investigated had a mean particle size between 135 and 145 nm and a narrow size distribution (PD<0.1).

3.2. Cellular association

OVCAR-3 cells were incubated with different concentrations of Rhodamine-PE labeled TAT-liposomes or control liposomes lacking the TAT-peptide. Fig. 1 shows that

Table 1
Characteristics of liposome preparations studied

Liposome formulation	Lipophilic fluorescent label	Hydrophilic fluorescent label	Mean particle size (nm)	PD[a]
TAT-liposomes	DiD	FITC-dextran	140	0.09
Control liposomes	DiD	FITC-dextran	135	0.04
TAT-liposomes	Rho-PE	–	145	0.05
Control liposomes	Rho-PE	–	140	0.06

[a] Polydispersity: indication of the size distribution of the liposomes; ranges from 0.0 for a monodisperse to 1.0 for an entirely heterodisperse suspension.

coupling of the TAT-peptide to the outer surface of the liposomes strongly increased the cellular association of the liposomes with OVCAR-3 cells.

3.3. Fixation-induced artifact

The influence of fixation techniques on the cellular distribution of fluorescently labeled TAT-liposomes has not been published yet, while it has been demonstrated recently by various research groups that fixation procedures have a major influence on the cellular localization of fluorescently labeled CPP [12,13,19]. Fig. 2 shows confocal microscopy images of living (Fig. 2A) and fixed (Fig. 2B) OVCAR-3 cells after a 1 h incubation with Rhodamine-PE labeled TAT-liposomes. After fixation with 4% formaldehyde (Fig. 2B), the fluorescence appeared in a diffuse pattern throughout the cytosol. No fluorescence was observed in the nucleus. When living OVCAR-3 cells were directly visualized (Fig. 2A), no intracellular localization was observed but the fluorescent TAT-liposomes were predominantly localized at the plasma membranes of the cells. Control liposomes could not be detected using the same photomultiplier settings (data not shown). These results illustrate that fixation procedures need to be avoided when studying cellular localization of TAT-liposomes as otherwise misleading results can be obtained.

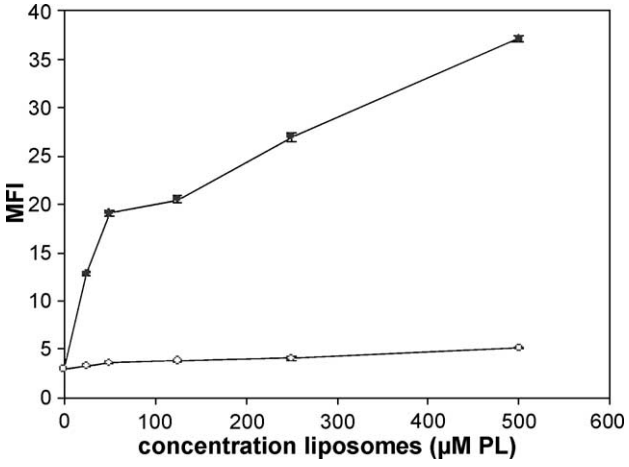

Fig. 1. Coupling of TAT-peptide to the outer surface of liposomes increases the cellular association with OVCAR-3 cells. Cells were incubated with different concentrations of Rho-PE labeled control liposomes (○) or TAT-liposomes (●) for 1 h at 4 °C, washed and analyzed by flow cytometry. Each point represents the mean fluorescence intensity (MFI) of 5000 cells analyzed and error bars indicate standard deviation (n=3).

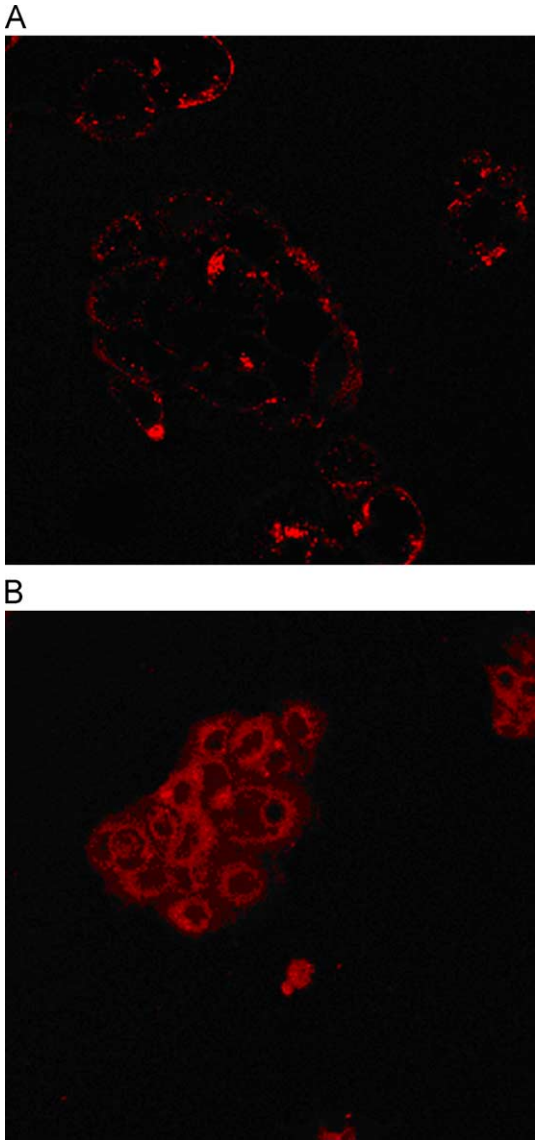

Fig. 2. Fixation induced redistribution of liposomal label. OVCAR-3 cells were incubated for 1 h at 37 °C with TAT-liposomes labeled with Rho-PE and either visualized without fixation (A) or after fixation with 4% formaldehyde (B).

3.4. Intracellular localization

Knowing the detrimental effects of fixation on cellular localization of TAT-liposomes, *living* OVCAR-3 cells were used in all subsequent experiments. Using confocal microscopy, the cellular localization of double-labeled TAT-liposomes and control liposomes after 1 or 24 h of incubation was studied.

To examine the liposome integrity during the experiments, both the liposomal bilayer and the aqueous core were fluorescently labeled with DiD and FITC-dextran, respectively. Co-localization of both liposomal labels would be indicative of the presence of intact liposomes. In addition, endosomes and lysosomes were labeled with Lysotracker Red, a compound known to localize primarily in the acidic compartments of cells [17].

After 1 h of incubation both liposomal labels were localized at the plasma membrane of the OVCAR-3 cells, which represents cell-bound intact TAT-liposomes (Fig. 3A). Endosomes and lysosomes were stained red with Lysotracker Red. An electronically merged image (right panel, Fig. 3A) shows no evidence of co-localization of the liposomal labels with Lysotracker Red. However, after 24 h of incubation, both liposomal labels were present intracellularly in a punctuate pattern (Fig. 3B). When these images are electronically merged with the confocal image visualizing Lysotracker Red staining, co-localization of the liposomal labels with the endosomal/lysosomal marker is clearly visible (right panel, Fig. 3B). From this co-localization, it can be concluded that the liposomes were present in endocytic vesicles and presumably were taken up by an endocytic process.

No binding or uptake was observed when control liposomes (lacking TAT-peptide) were incubated with OVCAR-3 cells for 1 or 24 h (data not shown).

3.5. Effect of low temperature and inhibitors

A punctuate intracellular distribution of Rho-PE labeled TAT-liposomes was observed when living OVCAR-3 cells in suspension were incubated for 5 h at 37 °C with TAT-liposomes and directly thereafter visualized using confocal laser scanning microscopy (Fig. 4A). When the 5 h incubation was performed at 4 °C, liposome-associated fluorescence was observed only at the plasma membrane of OVCAR-3 cells (Fig. 4B). The presence of the metabolic inhibitor iodoacetamide (Fig. 4C) or the endocytosis inhibitor cytochalasin D (Fig. 4D) in the incubation medium inhibited the uptake of TAT-liposomes at 37 °C by OVCAR-3 cells as only membrane-bound

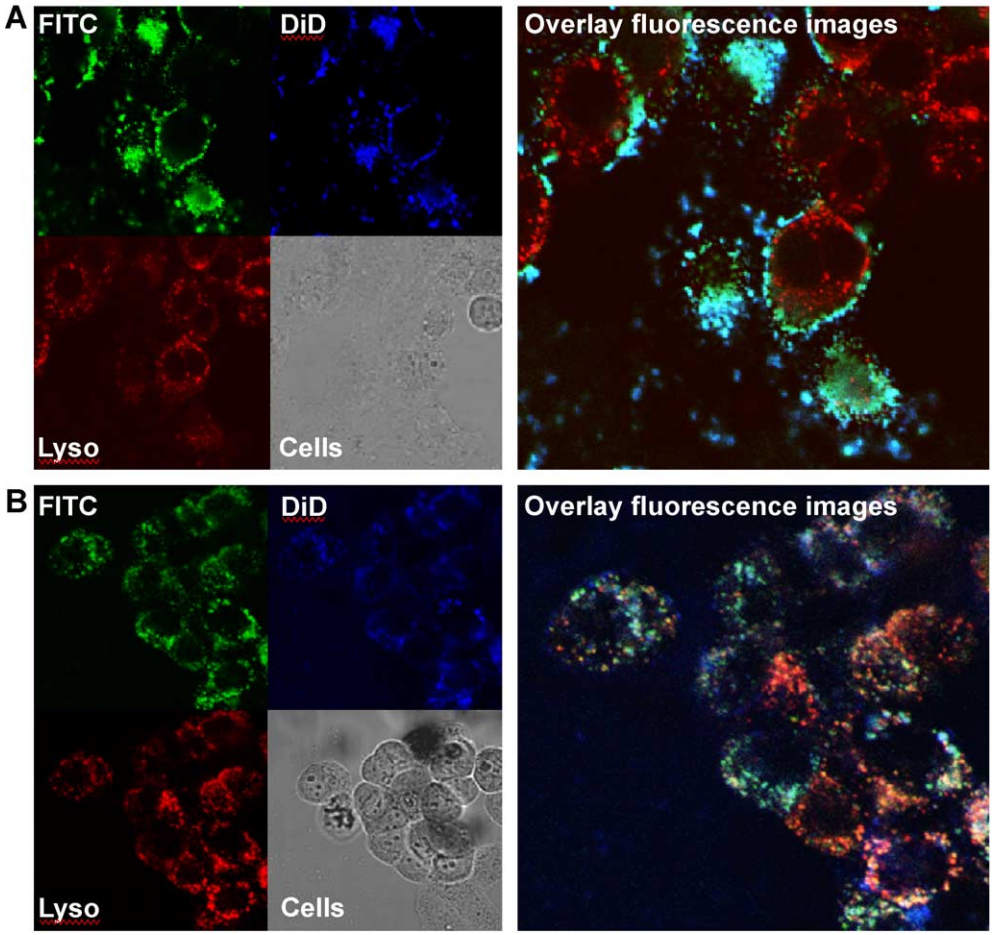

Fig. 3. Intracellular localization of TAT-liposomes. OVCAR-3 cells were incubated with 150 nmol of TAT-liposomes for 1 h and directly visualized (A) or subsequently incubated for 23 h without liposomes (B). Endosomes and lysosomes were stained 30 min prior to visualization with Lysotracker Red. In the right panels, the different confocal images are electronically merged.

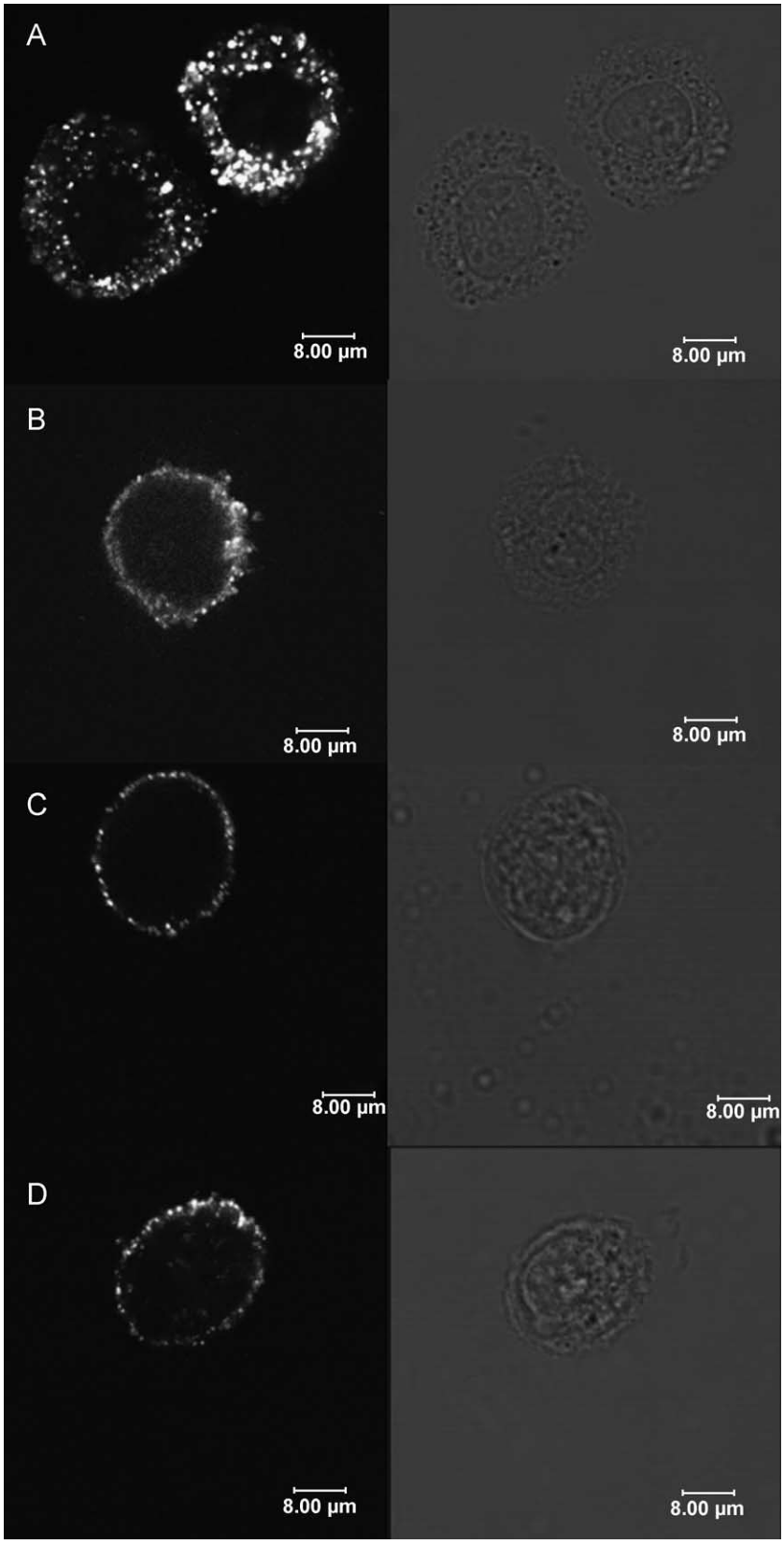

Fig. 4. Low temperature and metabolic inhibitors prevent uptake of TAT-liposomes by living OVCAR-3 cells. OVCAR-3 cells were incubated with TAT-liposomes for 5 h at 37 °C (A, C, D) or at 4 °C (B). Left panels are confocal images, right panels are phase contrast images. (A) Control, vesicular localization of TAT-liposomes; (B) incubation at 4 °C, plasma membrane binding of TAT-liposomes; (C) in the presence of iodoacetamide, plasma membrane binding of TAT-liposomes; (D) in the presence of cytochalasin D, plasma membrane binding of TAT-liposomes.

fluorescence was detected (Fig. 4C). Control liposomes were not taken up by OVCAR-3 cells after a 5 h incubation at 37 °C (data not shown).

To exclude the possibility that cellular uptake of TAT-liposomes in the presence of metabolic or endocytosis inhibitors cannot be visualized due to reduced binding of the TAT-liposomes to cells, cellular association in the absence or presence of inhibitor was studied by flow cytometry. Incubations were performed at 4 °C, which, as demonstrated in Fig. 4B, only resulted in binding to the plasma membrane since cellular uptake does not occur at this temperature. Fig. 5 shows that plasma membrane binding of TAT-liposomes to OVCAR-3 cells was not reduced due to the presence of iodoacetamide or cytochalasin D in the incubation medium.

3.6. Effect of polyanions

Recently, cell-surface exposed proteoglycans have been shown to play a role in the binding of the TAT-peptide to the cellular surface [27]. In addition, several studies have shown that the TAT-peptide interacts with numerous soluble polyanions, like heparin, heparan sulfate and pentosan sulfate [21–23]. The presence of those polyanions reduces the cellular uptake of the TAT-peptide.

The effect of two of these polyanions, heparin and dextran sulfate, present in the incubation medium, on the binding of TAT-liposomes to OVCAR-3 cells is shown in Fig. 6. As no significant cellular uptake occurs at 4 °C (shown in Fig. 4B), plasma membrane binding can be studied at this temperature. Both heparin and dextran sulfate reduced the binding of TAT-liposomes to OVCAR-3 cells in a concentration-dependent fashion (Fig. 6), heparin being somewhat more effective than dextran sulfate. These results indicate that glycosaminoglycans present on the cell surface are involved in the binding of TAT-liposomes to the plasma membrane of OVCAR-3 cells.

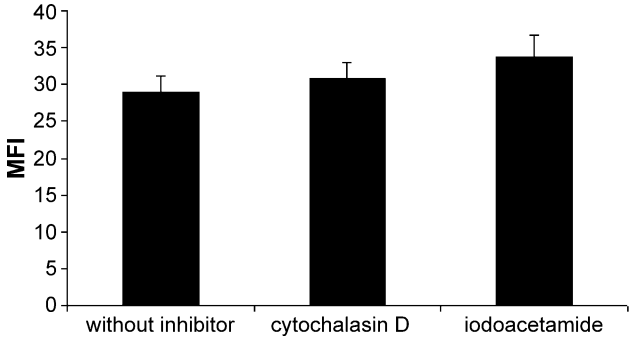

Fig. 5. Uptake inhibitors do not influence the binding of TAT-liposomes to OVCAR-3 cells. OVCAR-3 cells were incubated for 1 h at 4 °C with Rho-PE labeled TAT-liposomes, washed and analyzed by FACS. Cell-associated fluorescence is depicted as mean fluorescence intensity (MFI). Error bars represent the mean±standard deviation (n=3). Cellular association is not decreased due to the presence of inhibitors.

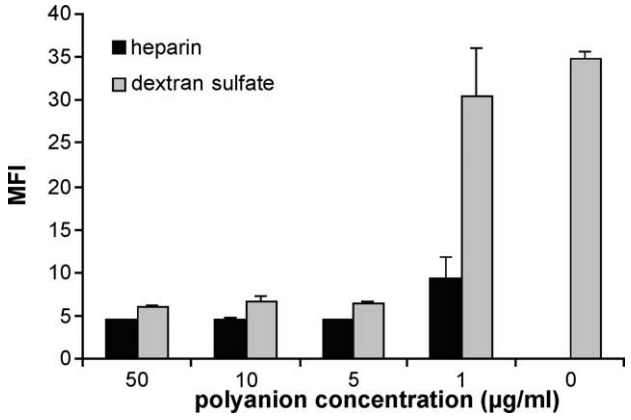

Fig. 6. Heparin and dextran sulfate reduce cellular association of TAT-liposomes to OVCAR-3 cells. OVCAR-3 cells were incubated for 1 h at 4 °C with Rho-PE labeled TAT-liposomes in the presence of different concentrations heparin or dextran sulfate. Cells were washed twice and analyzed by FACS for cell-associated fluorescence which is depicted as mean fluorescence intensity (MFI). Error bars represent the mean±standard deviation (n=3).

4. Discussion

Direct cytosolic delivery of liposomal macromolecular drugs, rather than uptake via endocytosis would be advantageous as degradation of encapsulated macromolecules in the lysosomal compartments is prevented. It was recently reported that direct cytosolic delivery of liposomes could be realized by coupling the TAT-peptide to the outer surface of the liposomes [25,26]. Translocation over the plasma membrane was suggested as uptake mechanism for TAT-liposomes as the uptake mechanism was considered to be time-, receptor- and energy-independent [25,26]. However, the results presented herein demonstrate that endocytosis rather than plasma membrane translocation is the underlying mechanism of cellular uptake of TAT-liposomes [25,26].

Coupling the TAT-peptide to the outer surface of liposomes strongly increases the binding of liposomes to OVCAR-3 cells (Fig. 1). It has been observed by others that the TAT-protein can enter a wide range of different cell types and that soluble heparin inhibits the biological activity of TAT-protein [21–23]. The latter observation raised the hypothesis that cell surface proteoglycans are involved in the uptake mechanism [27], which was supported by the finding that soluble heparin and dextran sulfate could inhibit binding of TAT-peptide to cells [27]. Moreover, TAT-peptide is unable to bind to cells genetically defective in the biosynthesis of fully sulfated heparan sulfate proteoglycans [27]. Fig. 6 shows that the presence of heparin or dextran sulfate almost completely reduces the degree of binding of TAT-liposomes to OVCAR-3 cells to the level of control liposomes, lacking the TAT-peptide. This indicates that cell

surface proteoglycans are involved in the binding of TAT-liposomes to cells as was also suggested for TAT-peptides coupled to a small fluorescent cargo [27].

When living OVCAR-3 cells were visualized after a 1-h of incubation with double-labeled TAT-liposomes, binding of intact TAT-liposomes to the plasma membrane of the cells was observed. After 24 h of incubation, both fluorescent labels co-localized with Lysotracker Red, a marker for endosomal and lysosomal compartments. This indicates that TAT-liposomes are taken up in an intact form by an endocytic pathway rather than via plasma membrane translocation. For fluorescently labeled CPP, it has already been discussed by various researchers that the cellular uptake occurs by endocytosis [2,3,5,8,19]. Endocytosis as the route of uptake for TAT-liposomes is further supported by the data shown in Fig. 4. At 4 °C or in the presence of the metabolic inhibitor iodoacetamide or the endocytosis inhibitor cytochalasin D, only membrane binding and no uptake of TAT-liposomes was observed, in contrast to incubation at 37 °C where liposomes are present intracellularly in vesicles.

The difference in results presented here and previously reported for the cellular uptake of TAT-liposomes [25,26] is likely explained by artifacts produced during fixation, which was avoided in these studies.

We clearly show that fixation of TAT-liposome-incubated cells caused a redistribution of liposomal label across the plasma membrane and a corresponding misinterpretation of microscopy data (Fig. 3). These results are in line with other reports indicating that fixation procedures can result in redistribution of fluorescently labeled CPP in cells [12,19].

In conclusion, TAT-peptide-mediated uptake of liposomes occurs via endocytosis rather than membrane translocation. This implies that TAT-liposomes do not have an advantageous mechanism of cell entry over other targeted drug delivery systems and that encapsulated drugs are still exposed to the degrading environment in the lysosomes. Nevertheless, extent of endocytic uptake is enhanced using TAT-peptides covalently coupled to liposomes, which may be intrinsically beneficial. In particular, in combination with endosomal escape promoters, such as virus-derived fusogenic peptides, which may further enhance cytosolic delivery of encapsulated macromolecules. Similar concepts are described in literature for endosomal escape of immunoliposomal drugs [14] and of TAT-fusion proteins [31].

References

[1] A. Astriab-Fisher, D. Sergueev, M. Fisher, B.R. Shaw, R.L. Juliano, Conjugates of antisense oligonucleotides with the Tat and antennapedia cell-penetrating peptides: effects on cellular uptake, binding to target sequences, and biologic actions, Pharm. Res. 19 (2002) 744–754.

[2] S. Console, C. Marty, C. Garcia-Echeverria, R. Schwendener, K. Ballmer-Hofer, Antennapedia and HIV TAT 'protein transduction domains' promote endocytosis of high Mr cargo upon binding to cell surface glycosaminoglycans, J. Biol. Chem. (2003).

[3] G. Drin, S. Cottin, E. Blanc, A.R. Rees, J. Temsamani, Studies on the internalisation mechanism of cationic cell-penetrating peptides, J. Biol. Chem. (2003).

[4] S. Fawell, J. Seery, Y. Daikh, C. Moore, L.L. Chen, B. Pepinsky, J. Barsoum, Tat-mediated delivery of heterologous proteins into cells, Proc. Natl. Acad. Sci. U. S. A. 91 (1994) 664–668.

[5] A. Fittipaldi, A. Ferrari, M. Zoppe, C. Arcangeli, V. Pellegrini, F. Beltram, M. Giacca, Cell membrane lipid rafts mediate caveolar endocytosis of HIV-1 Tat fusion proteins, J. Biol. Chem. 278 (2003) 34141–34149.

[6] T.C. Hamilton, R.C. Young, W.M. McKoy, K.R. Grotzinger, J.A. Green, E.W. Chu, J. Whang-Peng, A.M. Rogan, W.R. Green, R.F. Ozols, Characterization of a human ovarian carcinoma cell line (NIH:OVCAR-3) with androgen and estrogen receptors, Cancer Res. 43 (1983) 5379–5389.

[7] G.A. Koning, H.W. Morselt, M.J. Velinova, J. Donga, A. Gorter, T.M. Allen, S. Zalipsky, J.A. Kamps, G.L. Scherphof, Selective transfer of a lipophilic prodrug of 5-fluorodeoxyuridine from immunoliposomes to colon cancer cells, Biochim. Biophys. Acta 1420 (1999) 153–167.

[8] S.D. Kramer, H. Wunderli-Allenspach, No entry for TAT(44–57) into liposomes and intact MDCK cells: novel approach to study membrane permeation of cell-penetrating peptides, Biochim. Biophys. Acta 1609 (2003) 161–169.

[9] B. Lebleu, Delivering information-rich drugs-prospects and challenges, Trends Biotechnol. 14 (1996) 109–110.

[10] M. Lewin, N. Carlesso, C.H. Tung, X.W. Tang, D. Cory, D.T. Scadden, R. Weissleder, Tat peptide-derivatized magnetic nanoparticles allow in vivo tracking and recovery of progenitor cells, Nat. Biotechnol. 18 (2000) 410–414.

[11] M. Lindgren, M. Hallbrink, A. Prochiantz, U. Langel, Cell-penetrating peptides, Trends Pharmacol. Sci. 21 (2000) 99–103.

[12] M. Lundberg, M. Johansson, Positively charged DNA-binding proteins cause apparent cell membrane translocation, Biochem. Biophys. Res. Commun. 291 (2002) 367–371.

[13] M. Lundberg, S. Wikstrom, M. Johansson, Cell surface adherence and endocytosis of protein transduction domains, Mol. Ther. 8 (2003) 143–150.

[14] E. Mastrobattista, G.A. Koning, L. Van Bloois, A.C. Filipe, W. Jiskoot, G. Storm, Functional characterization of an endosome-disruptive peptide and its application in cytosolic delivery of immunoliposome-entrapped proteins, J. Biol. Chem. 277 (2002) 27135–27143.

[15] H. Nagahara, A.M. Vocero-Akbani, E.L. Snyder, A. Ho, D.G. Latham, N.A. Lissy, M. Becker-Hapak, S.A. Ezhevsky, S.F. Dowdy, Transduction of full-length TAT fusion proteins into mammalian cells: TAT-p27Kip1 induces cell migration, Nat. Med. 4 (1998) 1449–1452.

[16] F. Olson, C.A. Hunt, F.C. Szoka, W.J. Vail, D. Papahadjopoulos, Preparation of liposomes of defined size distribution by extrusion through polycarbonate membranes, Biochim. Biophys. Acta 557 (1979) 9–23.

[17] R.D. Palmiter, T.B. Cole, S.D. Findley, ZnT-2, a mammalian protein that confers resistance to zinc by facilitating vesicular sequestration, EMBO J. 15 (1996) 1784–1791.

[18] A. Prochiantz, Messenger proteins: homeoproteins, TAT and others, Curr. Opin. Cell Biol. 12 (2000) 400–406.

[19] J.P. Richard, K. Melikov, E. Vives, C. Ramos, B. Verbeure, M.J. Gait, L.V. Chernomordik, B. Lebleu, Cell-penetrating peptides: a re-evaluation of the mechanism of cellular uptake, J. Biol. Chem. (2002).

[20] G. Rouser, S. Fkeischer, A. Yamamoto, Two dimensional then layer chromatographic separation of polar lipids and determination of phospholipids by phosphorus analysis of spots, Lipids 5 (1970) 494–496.

[21] M. Rusnati, D. Coltrini, P. Oreste, G. Zoppetti, A. Albini, D. Noonan, F. d'Addadi Fagagna, M. Giacca, M. Presta, Interaction of HIV-1 Tat

protein with heparin. Role of the backbone structure, sulfation, and size, J. Biol. Chem. 272 (1997) 11313–11320.
[22] M. Rusnati, G. Tulipano, D. Spillmann, E. Tanghetti, P. Oreste, G. Zoppetti, M. Giacca, M. Presta, Multiple interactions of HIV-I Tat protein with size-defined heparin oligosaccharides, J. Biol. Chem. 274 (1999) 28198–28205.
[23] M. Rusnati, G. Tulipano, C. Urbinati, E. Tanghetti, R. Giuliani, M. Giacca, M. Ciomei, A. Corallini, M. Presta, The basic domain in HIV-1 Tat protein as a target for polysulfonated heparin-mimicking extracellular Tat antagonists, J. Biol. Chem. 273 (1998) 16027–16037.
[24] S.R. Schwarze, A. Ho, A. Vocero-Akbani, S.F. Dowdy, In vivo protein transduction: delivery of a biologically active protein into the mouse, Science 285 (1999) 1569–1572.
[25] V.P. Torchilin, R. Rammohan, V. Weissig, T.S. Levchenko, TAT peptide on the surface of liposomes affords their efficient intracellular delivery even at low temperature and in the presence of metabolic inhibitors, Proc. Natl. Acad. Sci. U. S. A. 98 (2001) 8786–8791.
[26] Y.L. Tseng, J.J. Liu, R.L. Hong, Translocation of liposomes into cancer cells by cell-penetrating peptides penetratin and tat: a kinetic and efficacy study, Mol. Pharmacol. 62 (2002) 864–872.
[27] M. Tyagi, M. Rusnati, M. Presta, M. Giacca, Internalization of HIV-1 tat requires cell surface heparan sulfate proteoglycans, J. Biol. Chem. 276 (2001) 3254–3261.
[28] M.H. Vingerhoeds, P.A. Steerenberg, J.J. Hendriks, D.J. Crommelin, G. Storm, Targeted delivery of diphtheria toxin via immunoliposomes: efficient antitumor activity in the presence of inactivating anti-diphtheria toxin antibodies, FEBS Lett. 395 (1996) 245–250.
[29] M.H. Vingerhoeds, P.A. Steerenberg, J.J. Hendriks, L.C. Dekker, Q.G. Van Hoesel, D.J. Crommelin, G. Storm, Immunoliposome-mediated targeting of doxorubicin to human ovarian carcinoma in vitro and in vivo, Br. J. Cancer 74 (1996) 1023–1029.
[30] E. Vives, P. Brodin, B. Lebleu, A truncated HIV-1 Tat protein basic domain rapidly translocates through the plasma membrane and accumulates in the cell nucleus, J. Biol. Chem. 272 (1997) 16010–16017.
[31] J.S. Wadia, R.V. Stan, S.F. Dowdy, Transducible TAT-HA fusogenic peptide enhances escape of TAT-fusion proteins after lipid raft macropinocytosis, Nat. Med. 10 (2004) 310–315.